ISBN: 978-3-95450-248-6 ISSN: 2673-5490 doi: 10.18429/JACoW-IPAC25-WEPM099

INVESTIGATION OF THE MICROWAVE INSTABILITY AT MAX IV LABORATORY IN COMBINATION WITH INTRA-BEAM SCATTERING

M. Brosi*, Å. Andersson, J. Breunlin, and F. Cullinan
Lund University - MAX IV, Lund, Sweden

Abstract

With the increasingly challenging parameters in 4th generation synchrotron light sources, collective effects causing instabilities are putting even stronger limitations on the area of stable operation. The microwave instability (MWI) is a longitudinal single-bunch instability driven by the geometric and the resistive-wall impedances. While the instability typically does not result in a beam loss, the resulting turbulent dynamics are accompanied by an increased energy spread and therefore deteriorate the light source performance. The threshold current depends on different beam parameters and can, without mitigation, for recently upgraded or currently under design light sources, be as low as or lower than the intended design current per bunch. At the same time, the instability threshold is also influenced by other collective effects such as the intra-beam scattering (IBS). The influence of the IBS on the microwave instability has been studied for the 3 GeV storage ring at the MAX IV laboratory. The presented experimental results show the expected influence on the MWI threshold by the coupling strength due to the resulting changes in the IBS.

INTRODUCTION

For ultra-low emittance rings, intra-beam scattering (IBS) is a common effect which can lead to an increase in bunch length, energy spread and horizontal emittance. The influence of IBS can be reduced by increasing the coupling between the vertical and horizontal plane, as this reduces the charge density in the transverse distribution. This is furthermore beneficial for the lifetime. At the same time, it is preferable to keep the vertical emittance below the diffraction limit. For the standard operation, a compromise is found.

Reducing the influence of IBS can affect other collective effects. Here, the influence of different coupling strength, and therefore different IBS strength, on the microwave instability (MWI) is measured. The MWI is a longitudinal single-bunch instability driven by the geometric and the resistive-wall impedances. The instability leads to a turbulent beam dynamic above the threshold with increases in energy spread, bunch length and, via the dispersion, horizontal emittance. The threshold current depends on beam parameters and impedance. For the 3 GeV storage ring at the MAX IV Laboratory [1], the threshold is currently above the design bunch current during standard operation. For the planned upgrade MAX $4^{\underline{U}}$ [2], the threshold will be reduced due to the reduction in the momentum-compaction factor.

As mentioned, the IBS also leads to a bunch lengthening and therefore will affect the MWI threshold. This has been investigate at e.g. the NSLSII [3] before. Here we present our measurements conducted at the 3 GeV ring a 4th generation synchrotron light source of the MAX IV Laboratory.

* miriam.brosi@kit.edu, now at KIT, Karlsruhe, Germany

Table 1: Beam Parameters

Parameters	Values
RF frequency / MHz	100
RF voltage / kV	1040
Synchrotron freq. / Hz	940
Beam energy / GeV	3
Long. damping time / ms	25.6
Natural bunch length (rms) / ps	40.8

MEASUREMENTS

The presented experiments were conducted during dedicated machine study shifts when it is possible to operate in single bunch mode as well as change different machine parameters, such as the acceleration voltage in the main cavities or adjust the coupling between the transverse planes. The coupling can be adjusted with the use of skew quadrupoles that are implemented as secondary windings on sextupole and octupole magnets. In the context of the presented measurements, the secondary windings on the horizontal octupoles ("oxx") were used.

To observe the change in coupling, the transverse emittances are monitored. They are calculated via the measured transverse beam sizes and the betatron functions plus the dispersion at the position of measurement. The bunch sizes are measured at two visible to near-UV light diagnostic beam lines [4] in an interferometric setup at positions with different values of the dispersion. The energy spread can be determined in the same way.

To measure the longitudinal bunch size, a streak camera with dual time-base is installed at one of the diagnostic beam lines. This allows the measurement of the longitudinal charge distribution on a turn-by-turn basis and therefore provides insight into the longitudinal dynamics in the presence of instabilities [5]. From the measured bunch profiles, the average bunch length is calculated. Additionally, to visualize the strength of the bunch-length fluctuations, the RMS of the bunch length over approx. 560 turns is calculated and averaged over 100 images taken 100ms apart. This value strongly increases at the MWI threshold when the bunch starts to experience dynamic deformations, making the threshold detection simple.

The resulting measurements for three different values of coupling (with $\varepsilon_y \approx 0.6\,\mathrm{pm\,rad}$, $\varepsilon_y \approx 2.3\,\mathrm{pm\,rad}$, and $\varepsilon_y \approx 32\,\mathrm{pm\,rad}$) are shown in Fig. 1 and the common beam parameters are given in Table 1.

ISBN: 978-3-95450-248-6 ISSN: 2673-5490 doi: 10.18429/JACoW-IPAC25-WEPM099

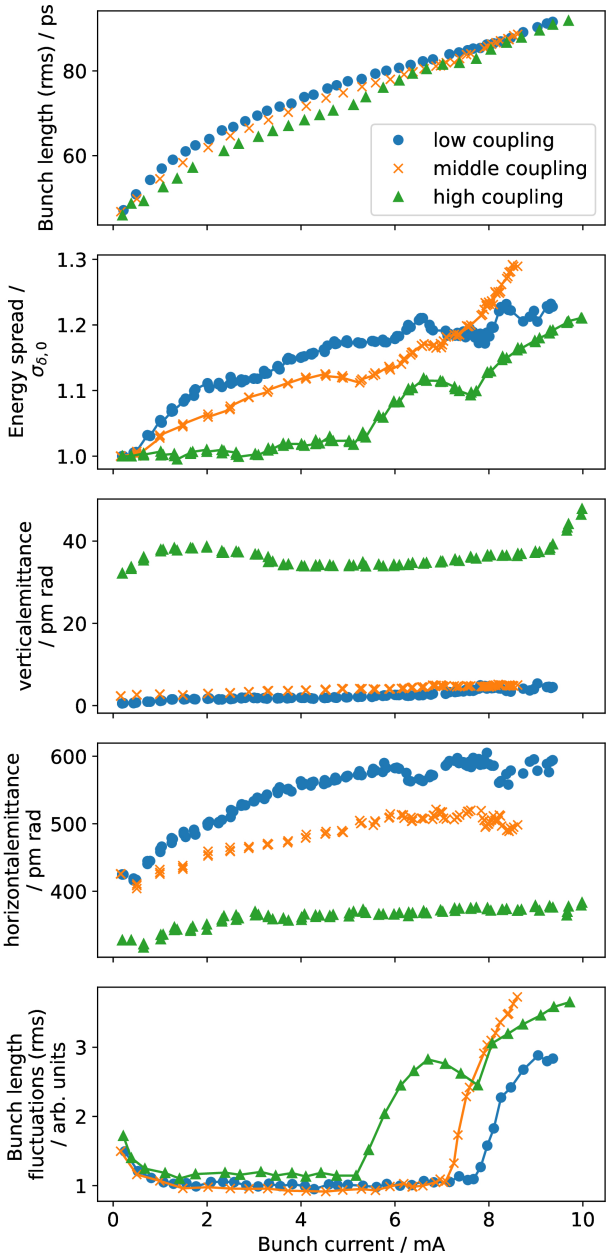

Figure 1: Measurement data taken at low coupling (blue), an intermediate value (orange) and high coupling (green). From top to bottom, the measured bunch length, energy spread, vertical emittance, horizontal emittance and bunch length fluctuations are displayed as function of the bunch current. The bunch length fluctuations increase strongly (visible as kink) at the instability threshold.

SIMULATION

To simulated the beam dynamics during the MWI, the Vlasov-Fokker-Planck solver Inovesa [6] has already been used in the past at MAX IV [5]. Inovesa is purely operating on the longitudinal phase space density and therefore does not provide an intrinsic calculation of the IBS effect.

Instead, the IBS was considered indirectly by emulating the effects on the beam. To this end, the natural bunch parameters where adjusted to current-dependent values derived from the measurements.

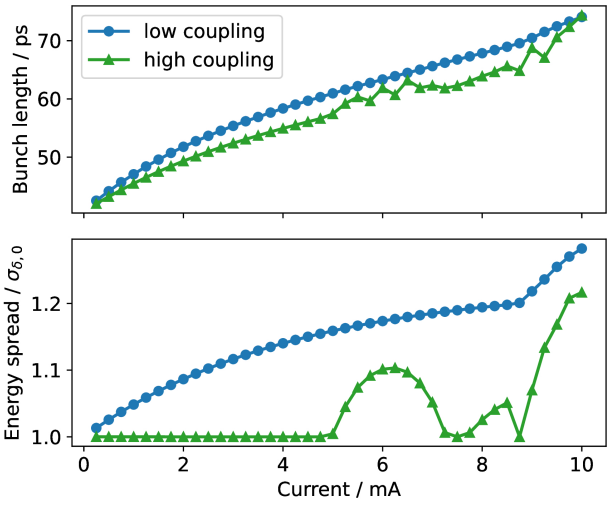

Figure 2: Vlasov-Fokker-Planck solver simulations of the microwave instability with the influence of IBS considered indirectly for the "low coupling" case and not considered for the "high coupling" case.

The growth in energy spread due to IBS was extracted from the measurements as a current-dependent factor. For each Inovesa simulation at a given bunch current, the natural energy spread was multiplied by the corresponding factor. The resulting increased energy spread was given into Inovesa as new "natural" energy spread. Additionally, from this adjusted energy spread a current-dependent "effective" damping time was extracted, which includes the additional current-dependent growth rate due to IBS. Based on the equation for the natural energy spread $\sigma_{\delta,0}$ [7]

$$\sigma_{\delta,0}^2 = \frac{55}{32\sqrt{3}} \left(\frac{\hbar}{m_e c}\right)^2 \left(\frac{E}{m_e c^2}\right)^2 \frac{I_3}{2I_2 - I_4}$$

and the equation for the longitudinal damping time τ_z

$$\tau_{z,0} = 2T_0 \frac{E}{U_0} \frac{1}{J_z} = \frac{4\pi T_0}{C_\gamma E^3 I_2 J_z} \quad \text{with} \quad J_z = 2 + \frac{I_4}{I_2}$$

the following proportionality can be derived

$$\sigma_{\delta,0}^2 = \frac{55}{32\sqrt{3}} \left(\frac{\hbar}{m_e c}\right)^2 \left(\frac{E}{m_e c^2}\right)^2 C_\gamma \frac{E^3}{4\pi T_0} I_3 \tau_{z,0},$$

where C_γ is Sand's constant, E is the beam energy, T_0 is the revolution time, I_x with $x = 2, 3, 4$ are the radiation integrals number two to four, $\hbar$ is the reduced Planck constant, m_e is the electron rest mass and c is the speed of light. For a constant beam energy this simplifies to

$$\sigma_{\delta,0} \propto \sqrt{\tau_{z,0}}.$$

Assuming the IBS growth rate acts as an additional current-dependent contribution to the equilibrium between quantum

ISBN: 978-3-95450-248-6 ISSN: 2673-5490 doi: 10.18429/JACoW-IPAC25-WEPM099

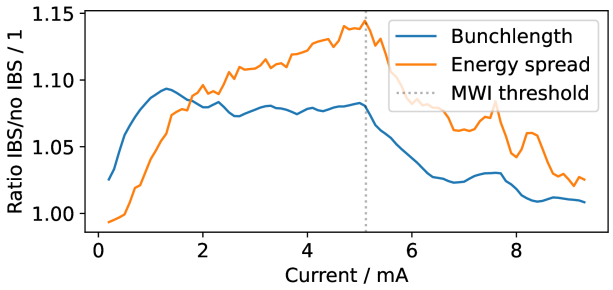

Figure 3: Ratio of measured energy spread and bunch length between the measurements at low coupling and at high coupling shown as a function of the bunch current. The instability threshold of the MWI (for the high coupling case) is shown as gray line.

excitation and radiation damping, this results in a new equilibrium energy spread. Using the natural energy spread and damping time, the "effective" damping time can be calculated from the measured energy spread as

$$\tau_{z,\mathrm{eff}}(I) = \frac{\sigma^2_{\delta,\mathrm{meas}}(I)}{\sigma^2_{\delta,0}}\tau_{z,0}.$$

For the simulation of the MWI the combination of the geometric impedance model [8] (GdfidL [9]) and the resistive wall impedance (including NEG coating, ImpedanceWake2D [10]) has been used. Two cases have been simulated. For one, the adjusted energy spread and damping time based on the low coupling measurements were used to show the influence of IBS. For the second case, no IBS was considered, which is assumed to correspond to the high coupling case in the measurements. The results are shown in Fig. 2.

The current-dependent influence of the IBS on the energy spread was cross-checked with the IBS module in mbtrack2 ("CIMP" and "Bane" algorithm) [11] and with the ZAP code [12]. Both codes return a slightly different but in both cases stronger influence than observed in the experiments. The differences will be investigated further and could originate in the decreased accuracy of the measurements for very low bunch currents, which were used as starting values for the simulations. Overall, it was therefore decided to use the measurement data as basis for the above described method of indirectly simulating the IBS influence with Inovesa.

RESULTS

The measurements in Fig. 1 show the bunch length, energy spread and transverse emittances for the three coupling strengths. The resulting change in IBS strength is clearly visible on all parameters and follows the expectations. The vertical emittance increases with increased coupling resulting in an decreased horizontal emittance. At increased coupling, also the current-dependent increase of the horizontal emittance is less pronounced. In the longitudinal plane, the expected additional bunch-lengthening with current is observed in the presence of IBS. And the energy spread shows a strong current-dependent increase already below the MWI instability for the low coupling case while remaining rather constant for the case with high coupling. The same is visible in the simulation results in 2.

Figure 3 shows the ratio between the measurements at low coupling vs high coupling for the bunch length and energy spread. Below the MWI threshold, the ratio increases continuously for the energy spread as it is nearly constant for the high coupling case. For the bunch length, the ratio first increases strongly due to IBS but flattens already at currents well below the MWI threshold due to the bunch-lengthening caused by the potential-well distortion. Above 5.3 mA, the ratios both start to decrease as the turbulent dynamic during the MWI increases bunch length and energy spread for the high coupling case while the low coupling case is still below its respective MWI threshold.

The MWI threshold can be seen very clearly in the measured bunch-length fluctuations. The thresholds range from 7.8±0.2 mA in the case with low coupling and therefore strong IBS contributions over 7.2±0.1 mA for the intermediate coupling case to 5.3±0.2 mA for the high coupling case where nearly no influence of the IBS is expected. This corresponds to an increase of the MWI threshold by nearly 50% for the low coupling case.

The simulations show qualitatively the same effect. The threshold increases from 4.75±0.125 mA to 8.75±0.125 mA when IBS is included. Also the bunch length shows qualitatively the same behaviour as in the measurements. Quantitatively, the overall bunch-lengthening is not as strong as in the measurements. Since this is also the case without the IBS added, it indicates that the impedance model needs to be investigated further. Nevertheless, the overall observations agree well and the expected influence of the IBS on the threshold of the MWI is clearly visible.

SUMMARY

The measurements of the MWI threshold current for different coupling strength show the expected influence of IBS, with low coupling leading to a stronger IBS and an increased threshold. The drawback is the increased horizontal emittance. The other way round, this also means that a common way to mitigate IBS (increasing coupling, e.g. [13]) can reduce the MWI threshold. To be able to use a purely longitudinal Vlasov-Fokker-Planck solver, the IBS was considered indirectly during simulations by adjusting the natural energy spread as well as the damping time based on the measurement. The resulting simulations show a good qualitative agreement with the experimental results.

For MAX IV (3 GeV ring), the threshold is already higher than the design bunch current during standard multi-bunch operation, so that the coupling can be chosen freely. For 4th generation light sources in general, the trade-off between IBS and the MWI threshold should be considered.

REFERENCES

[1] P. F. Tavares *et al.*, "Status of the MAX IV accelerators", in *Proc. IPAC'19*, Melbourne, Australia, May 2019. doi:10.18429/JACoW-IPAC2019-TUYPLM3

ISBN: 978-3-95450-248-6 ISSN: 2673-5490 doi: 10.18429/JACoW-IPAC25-WEPM099

[2] E. Al-Dmour *et al.*,"MAX 4U: an upgrade of the MAX IV 3 GeV ring", presented at the 16th International Particle Accelerator Conference, 2025, paper MOPS061, this conference.

[3] A. Blednykh *et al.*, "Combined effect of IBS and impedance on the longitudinal beam dynamics", in *Proc. IPAC'21*, Campinas, Brazil, May 2021, pp. 4274–4277. doi:10.18429/JACoW-IPAC2021-THPAB240

[4] J. Breunlin and Å. Andersson, "Emittance diagnostics at the MAX IV 3 GeV storage ring", in *Proc. IPAC'16*, Busan, Korea, May 2016, pp. 2908–2910. doi:10.18429/JACoW-IPAC2016-WEPOW034

[5] M. Brosi *et al.*, "Time-resolved measurement and simulation of a longitudinal single-bunch instability at the MAX IV 3 GeV ring", in *Proc. IPAC'23*, May 2023. doi:10.18429/jacow-ipac2023-wepa020

[6] Patrik Schönfeldt *et al.*, "/Inovesa: Fireworks (v1.1.2)", *Zenodo*, 2023. doi:10.5281/zenodo.7996461

[7] R. H. Helm, M. J. Lee, P. L. Morton, and M. Sands, "Evaluation of synchrotron radiation integrals", *IEEE Trans. Nucl. Sci.*, vol. 20, no. 3, pp. 900–901, 1973. doi:10.1109/TNS.1973.4327284

[8] M. Klein *et al.*, "Study of collective beam instabilities for the MAX IV 3 GeV ring", in *Proc. IPAC'13*, Shanghai, China, 2013. https://accelconf.web.cern.ch/ipac2013/papers/tupwa005.pdf

[9] W. Bruns, "The GdfidL Electromagnetic Field Simulator", http://www.gdfidl.de.

[10] N. Mounet *et al.*, CERN, BE dpt, Geneva, https://gitlab.cern.ch/IRIS/IW2D

[11] A. Gamelin *et al.*, "mbtrack2", *Zenodo*, v 0.8.0, Dec. 16, 2024. doi:10.5281/zenodo.14418989

[12] M. S. Zisman, S. Chattopadhyay, and J. J. Bisognano, "ZAP user's manual", Lawrence Berkeley Lab., CA, USA, Rep. LBL-21270; ESG-15, Dec. 1986.

[13] A. Vivoli *et al.*, "Intra-beam scattering effect in the SOLEIL storage ring upgrade", in *Proc. IPAC'19*, Melbourne, Australia, May 2019, pp. 3106–3108. doi:10.18429/JACoW-IPAC2019-WEPTS011